Open Archive Toulouse Archive Ouverte (OATAO)

OATAO is an open access repository that collects the work of some Toulouse researchers and makes it freely available over the web where possible.

This is an author's version published in: http://oatao.univ-toulouse.fr/20525

Official URL: https://doi.org/10.1016/j.biortech.2016.04.087

Any correspondance concerning this service should be sent to the repository administrator: tech-oatao@listes-diff.inp-toulouse.fr

Biocathodes reducing oxygen at high potential select biofilms dominated by Ectothiorhodospiraceae populations harboring a specific association of genes

Elie Desmond-Le Quéméner [a], Mickaël Rimboud [b], Arnaud Bridier [a], Céline Madigou [a], Benjamin Erable [b], Alain Bergel [b], Théodore Bouchez [a,*]
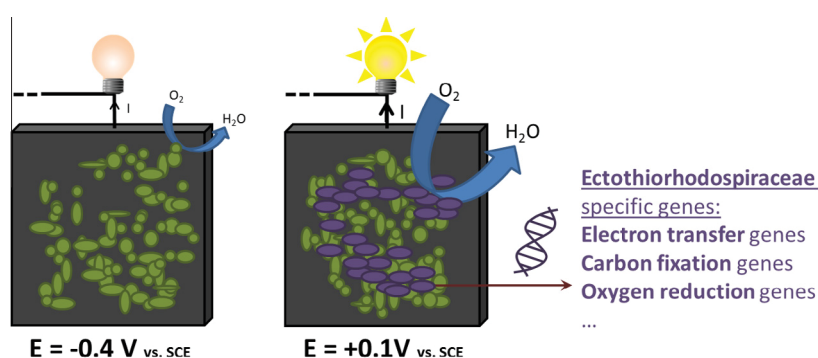
[a] Irstea, UR HBAN, 1 rue Pierre-Gilles de Gennes, 92761 Antony cedex, France
[b] Laboratoire de Génie Chimique (LGC), CNRS, Université de Toulouse (INPT), 4 allée Emile Monso, BP 84234, 31432 Toulouse, France

HIGHLIGHTS

- 10 biocathodes were formed at +0.1 V and −0.4 V vs. SCE.
- 4 biocathodes active at +0.1 V vs. SCE have been obtained.
- Most efficient cathodic biofilms are dominated by Ectothiorodospiraceae.
- The most efficient biofilm was characterized by shotgun metagenomics.
- Candidate genes implicated in electron transfer and autotrophic growth are outlined.

GRAPHICAL ABSTRACT

E = -0.4 V vs. SCE   E = +0.1V vs. SCE

Ectothiorhodospiraceae specific genes:
Electron transfer genes
Carbon fixation genes
Oxygen reduction genes
...

ABSTRACT

Biocathodes polarized at high potential are promising for enhancing Microbial Fuel Cell performances but the microbes and genes involved remain poorly documented. Here, two sets of five oxygen-reducing biocathodes were formed at two potentials (−0.4 V and +0.1 V vs. saturated calomel electrode) and analyzed combining electrochemical and metagenomic approaches. Slower start-up but higher current densities were observed at high potential and a distinctive peak increasing over time was recorded on cyclic voltamogramms, suggesting the growth of oxygen reducing microbes. 16S pyrotag sequencing showed the enrichment of two operational taxonomic units (OTUs) affiliated to Ectothiorodospiraceae on high potential electrodes with the best performances. Shotgun metagenome sequencing and a newly developed method for the identification of Taxon Specific Gene Annotations (TSGA) revealed Ectothiorhodospiraceae specific genes possibly involved in electron transfer and in autotrophic growth. These results give interesting insights into the genetic features underlying the selection of efficient oxygen reducing microbes on biocathodes.

1. Introduction

Microbial Fuel Cells (MFCs) are a promising technology that exploit the oxidative metabolism of electroactive microorganisms to extract electricity from the degradation of dissolved organic

* Corresponding author.
  E-mail address: theodore.bouchez@irstea.fr (T. Bouchez).

matter present in various natural media, such as wastewater, sewage sludges, industrial effluents (from brewery, paper mill manufacture…), sea or freshwater, soils. Even if promising results have been obtained in the laboratory, the practical applications of this technology are still limited mainly because of problems encountered at the cathode (Logan, 2009).

Reactions occurring at the cathode serve as sink for the electrons generated at the anode. Most commonly, oxygen is used at the cathode as electron acceptor because of its high availability and high reductive potential, even if the kinetics of oxygen reduction reactions (ORR) are very slow (Erable et al., 2012). To improve ORR's kinetics, metal catalysts such as platinum, manganese oxides, iron complexes and cobalt complexes have been used (Zhang et al., 2012b). Other specific materials, such as activated carbon, have also been developed to reduce the costs (Wei et al., 2011), but these electrodes remain expensive and subject to poisoning or fouling (Wei et al., 2011). As an alternative, microbes can be used at the cathode to catalyze ORR (Erable et al., 2012) in the same way as they are used to catalyze substrate oxidation at the anode. Contrary to metallic catalysts, the microbes are cheap and self-sustaining, but studies analyzing cathodic oxygen reducing microbes and the parameters influencing biofilm formation are still rare in comparison with what is available for bioanodes.

Few articles were dedicated to the study of the electrode potential effect on the biocathode performances (Liang et al., 2009; Ter Heijne et al., 2010; Xia et al., 2012). All of them found similar results indicating that low potentials allowed a fast startup but that highest currents were obtained at higher potentials, which is an interesting observation considering that higher cathodic potential leads to higher MFC power output. From an electrochemical point of view, Milner et al. evidenced a change in the biofilm voltammetric response that displayed one or two reductive signals depending on the polarization potential (respectively 97 and 397 mV vs. SHE) (Milner et al., 2014). Overall, the optimal potentials identified in these studies (Liang et al., 2009; Ter Heijne et al., 2010; Xia et al., 2012) were all found in a similar range (242, 347 and 302 mV vs. standard hydrogen electrode (pH 0) (SHE) respectively). The biochemical processes occurring at such potentials were investigated by Wang et al. (2015) who used a combination of metagenomics and metaproteomics. They found that members of the bacterial family Chromatiaceae were expressing an autotrophic CO_2 fixation pathway and several proteins potentially involved in extracellular electron transfer (EET) mechanisms. Besides Chromatiaceae, Xia et al. also reported a selection of two dominant clones, one belonging to the phylum Bacteroidetes and the other to the genus *Thiorhodospira* (a γ-proteobacteria) at 302 mV vs. SHE (Xia et al., 2012). However, the reasons why a high potential boosts the electrochemical activity of a complex microbial community remain unclear considering that the energy available for microbial growth decreases as the potential increases.

The main objective of this work is therefore to give more insights into the mechanisms leading to the selection of microbial populations that are efficient in reducing oxygen at high potential. For this, a selection experiment was designed using two groups of five oxygen reducing biocathodes formed from compost leachate. Electrodes of the first group were polarized at a deliberately low potential (−0.4 V vs. saturated calomel electrode (SCE) = −158 mV vs. SHE) to allow the development of a wide range of cathodic microbial communities (Cournet et al., 2010b). Electrodes of the second group were polarized at a potential encompassed within the optimal range mentioned above (Liang et al., 2009; Ter Heijne et al., 2010; Xia et al., 2012) (+0.1 V vs. SCE = 342 mV vs. SHE). The biocathodes dynamics were characterized by electrochemistry methods such as chronoamperometry and cyclic voltammetry. The microbial community composition obtained at both potentials was investigated using high throughput 16S rRNA gene sequencing, evidencing the selection of particular phylotypes in cathodic biofilms at high potential. A shotgun metagenomic experiment was then performed followed by the identification of Taxon Specific Gene Annotations (TSGA).

2. Materials and methods

2.1. Electrochemical cell, medium and test

The electrochemical cell was a classical one compartment cell with a three electrode set-up adapted from a 500 ml Schott vial (Supplementary Material Figure S1). The working electrode was a 2 cm² carbon cloth (Paxitech®, France) electrode connected by a platinum wire, the counter-electrode a 10 cm² platinum grid and the reference electrode was a saturated calomel electrode (SCE). Unless otherwise stated, all potentials stated in this paper were recorded against the SCE reference electrode (242 mV vs. standard hydrogen electrode (pH 0) SHE).

Compost leachate was used as medium and inoculum. It was produced from commercially available garden compost (Eco-Terre®) using the method described elsewhere (Cercado et al., 2013) but without addition of acetate. As shown in the study by Cercado et al. this leachate constitutes an interesting source of electroactive microorganisms and a rustic growth medium (Cercado et al., 2013). All experiments were conducted in a stove with temperature controlled at 40 °C. Reactors were air-opened and experiments were conducted under quiescent conditions. No stirring or forced aeration were performed in order to not disturb the growth of the biofilm. The pH was measured every two days along the experiment. It didn't evolve significantly, varying from 7.6 in the compost leachate on day 0 to a mean of 8.2 ± 0.3 in the reactors at the end of experiment.

Electrochemical experiments were conducted using a multichannel potentiostat (Biologic, France) and the EC-Lab software. Microbial electrodes were formed under polarization by chronoamperometry, five electrodes (numbered 1 to 5) under −0.4 V during 14 days and five electrodes (numbered 6 to 10) under +0.1 V vs. SCE. Evolutions of the current density J in function of time were recorded for each reactor. The counter-electrode potentials were also measured all along the experiment. At some point during the chronoamperometry, cyclic voltammetry starting at the polarization potential and scanning from there to 0.3 V and back down to −0.6 V were realized at scan rate 1 mV s⁻¹. Three voltammograms were recorded each time. The three voltammograms were similar, and the second one was chosen to be presented in the figures. At some point, gases (nitrogen, air or oxygen) were temporarily supplied in the cell through a tube immersed in the electrolyte (Supplementary Material Figure S1). Nitrogen was supplied from a commercial bottle of pure nitrogen (Linde gas®, 4.5 purity), air was brought using an aquarium pump and oxygen using an electrolysis cell. At the end of experiment, a sample of each reactor medium together with each carbon cloth electrode were taken off and frozen for later population analysis.

2.2. Pyrotags sequencing

The bacterial populations of the cathodic biofilms were analyzed using 16S rDNA-pyrotags sequencing. DNA was extracted, quantified and checked for quality as described in a previous work (Rimboud et al., 2015). DNA samples were sent to Research and Testing Laboratory (RTL – Texas, USA) where 454 pyrosequencing (Roche) with 28F (5′-*GAG TTT GAT YMT GGC TC*-3′) and 519R (5′-*GWA TTA CCG CGG CKG CTG*-3′) primers was performed.

2.3. Metagenome shotgun sequencing

Metagenome shotgun sequencing was realized using the Ion Torrent Personal Genome Machine platform using manufacturer's protocols. Library was prepared from total DNA extracts using the Ion Xpress Plus Fragment Library Kit. Template preparation was carried out with the OneTouch 400 Template v2 kit and sequencing was performed using the Ion PGM HiQ Sequencing Kit (high sequencing accuracy) and Ion 316 v2 Chip kit. 3,370,101 reads were obtained representing a total throughput of 932 Mb with a median readlength of 280 bp.

2.4. Bioinformatics

16S pyrotags were analyzed with the open source software package QIIME (Caporaso et al., 2010) "Quantitative Insights Into Microbial Ecology" as detailed in a previous study (Rimboud et al., 2015). Taxonomic assignation was performed with the RDP classifier (Cole et al., 2009) trained on Silva 108 release set (Quast et al., 2013) using the most abundant sequence in each OTU as representative sequence and a bootstrap cut-off of 0.8.

Phyloseq and edgeR packages from R software were used for the detection of differentially abundants OTUs (McMurdie and Holmes, 2013; Robinson et al., 2010) in samples from electrodes relative to samples from liquid media.

For phylogenetic analyses, the selected representative sequences were processed as explained in a previous work (Rimboud et al., 2015). The final tree was computed with PhyML (Guindon and Gascuel, 2003) using the GTR model with optimized equilibrium frequencies, a gamma correction to take into account the heterogeneity of evolutionary rates across sites (four discrete classes of sites, an estimated alpha parameter and an estimated proportion of invariable sites) and SPR & NNI topology searches with five random starting trees.

Raw, unassembled reads obtained from metagenome shotgun sequencing were annotated with the online pipeline MG-RAST (Meyer et al., 2008) with default parameters. Features attributed to Ectothiorhodospiraceae were analyzed using the online workbench tool. Reads identified as rRNA were recovered and analyzed in our QIIME pipeline with the same parameters as for pyrotags.

3. Results and discussion

3.1. Electrochemical characterization of the biocathodes polarized at −0.4 V vs. SCE

The performance and lag times displayed by the five electrodes are indexed in Table 1 (electrodes numbered 1–5). A representative

Table 1
Compared performances of the biocathodes poised at −0.4 and +0.1 V vs. SCE, respectively. Chronoamperometric current densities at the end of the experiment are indicated in the third column; lag times to reach a current production of −5 mA m^{-2} for low potential electrodes or −10 mA m^{-2} for high potential electrodes are shown in the fourth column.

Polarization potential	Electrode number	J_{pol}/A m^{-2}	Lag time/days
−0.4 V vs. SCE	1	−0.16	1.8
	2	−0.22	1.2
	3	−0.12	2.1
	4	−0.18	1.3
	5	−0.14	1.7
+0.1 V vs. SCE	6	−0.17	10.1
	7	−0.15	9.8
	8	−0.11	10.0
	9	−0.40	7.1
	10	−0.05	–

chronoamperogramm obtained with the biocathodes polarized at −0.4 V vs. SCE is presented in Fig. 1A (biocathode number 3). The current started to decrease after a lag time of 2 days and reach a plateau that stabilized around −0.11 A m^{-2} on the 3rd day. It remained stable during 10 days. Then, at day 13.2, air was supplied to the cell. The current dropped immediately revealing that oxygen transfer was the limiting step in current production. It reached a minimum of −0.35 A m^{-2}, before coming back to the initial value of −0.11 A m^{-2} as air flux was stopped. The mean current density considering the five reactors under stationary conditions was −0.16 ± 0.04 A m^{-2} (Table 1).

After stabilization of the reduction current on day 3, the polarization was interrupted several times in order to record cyclic voltammograms on each biocathode. A representative cyclic voltammogram, realized at day 12.2 day with biocathode 3 is presented on Fig. 1B, together with the control performed at $t = 0$. It shows a typical signal attributable to oxygen reduction with a current wave starting around −0.2 V vs. SCE and a plateau of limiting current of −0.21 A m^{-2}. The voltammetric response was reproducible from one reactor to the other and remained stable all along the experiment after the biofilm formation. Limiting current densities measured on the reductive scan for each electrode ranged from −0.17 to −0.30 A m^{-2}, with a mean of −0.23 ± 0.05 A m^{-2}. Voltammogram were performed again on day 13.2 during the period of air supply. An enhanced response was observed (plain line, Fig. 1B). No plateau was observed and current densities were greatly increased by the faster O$_2$ transfer to the cathode surface. A maxi-
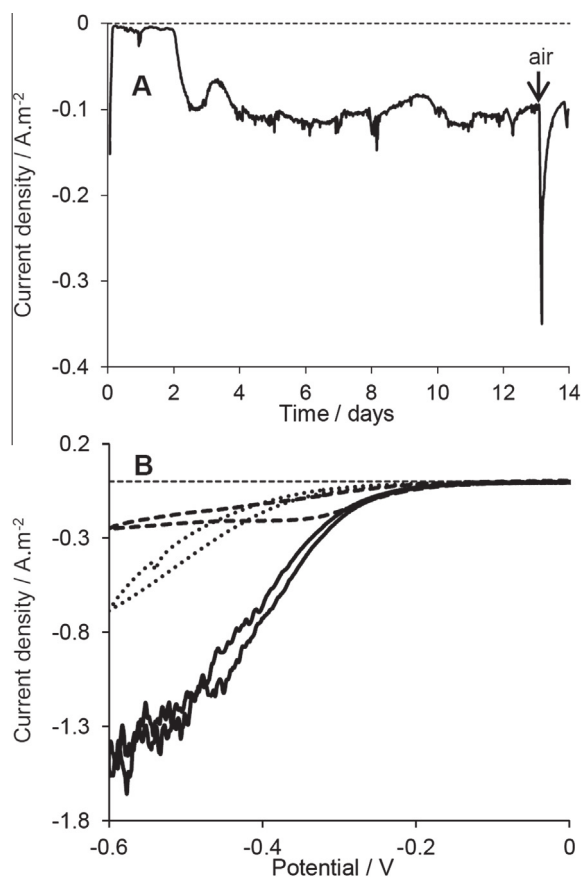

Fig. 1. Electrochemical characterization of the biocathode number 3 formed at −0.4 V vs. SCE. A: chronoamperometry, electrode polarized at −0.4 V. B: cyclic voltammograms of O$_2$ reduction by the biocathode: blank without catalysis at $t = 0$ (dotted line), in presence of a forced aeration (air supplied with an aquarium pump, plain line, day 13.2), and under normal condition (dashed line, day 8).

mum reduction current density of $-1.5 \, A \, m^{-2}$ was recorded at the lower limit of the scanned potential range ($-0.6 \, V$).

3.2. Electrochemical characterization of the biocathodes polarized at +0.1 V vs. SCE

The chronoamperometry with the shortest lag time recorded with an electrode polarized at +0.1 V vs. SCE (electrode 9) is presented on Fig. 2. A reduction current started to be observed after 6.7 days, down to $-0.17 \, A \, m^{-2}$ on day 11, before various tests were applied to the reactor (Fig. 2B). Contrary to what was observed with the biocathodes formed at -0.4 V vs. SCE, a continuous increase of the reduction current is observed to the end of the experiment on day 13.2. On day 11.2, air was forced for two hours in the reactor and current density dropped suddenly down to $-0.31 \, A \, m^{-2}$. After the air flow was stopped, it stabilized back to $-0.24 \, A \, m^{-2}$ on day 11.7. A deoxygenation of the medium by supplying nitrogen during 2.5 h reduced the reduction current to zero on day 11.9, showing that the current was due to oxygen reduction. An air flux followed immediately the nitrogen on day 12 and regenerated the reduction current, down to $-0.36 \, A \, m^{-2}$. Finally, two oxygen spargings of respectively 1 and 3 h on days 12.2 and 12.9 were applied. They enhanced the reduction current down to respectively -0.53 and $-0.67 \, A \, m^{-2}$, further confirming that oxygen was the electron acceptor at the cathode.

Concerning the other four electrodes formed at +0.1 V vs. SCE (electrodes 6, 7, 8, 10) a similar pattern was recorded except that

longer lag-times preceded the onset of oxygen reduction. The current densities measured by chronoamperometry for each electrode at the end of experiment (after 13.2 days) are reported in Table 1. For all reactors (1–10), maximal values measured for counter-electrode potentials were around +0.7 V vs. SCE. It indicated that the main anodic reaction was water oxidation to oxygen ($E = 0.573 \, V$ vs. SCE at pH 7).

Cyclic voltammetry were recorded at different times during the polarization of electrode 9. Voltammograms on days 0, 7 and 11.2 without gas supply are presented on Fig. 3A, whereas a voltammogram recorded on day 13 under oxygen supply, is presented on Fig. 3B. Voltammograms recorded under quiescent conditions (Fig. 3A) presented two different behaviors. On day 7, i.e. during the lag time observed by chronoamperometry, the curve showed a similar response than voltammograms previously recorded with electrodes polarized at -0.4 V vs. SCE ($-0.26 \, A \, m^{-2}$, -0.2 V vs. SCE). A contrario, voltammogram recorded on day 11.2, after current production began, presented a signal of similar intensity (peak current $-0.23 \, A \, m^{-2}$) but at a higher potential +0.2 V vs. SCE (Fig. 3A). This signal at +0.2 V vs. SCE was a distinctive feature that was observed with more or less intensity (depending on the lag time) with electrodes 6, 7, 8 and 9, i.e. with electrodes polarized at +0.1 V vs. SCE. The two signals (-0.2 and +0.2 V vs. SCE) were concomitantly present on the cyclic voltammograms recorded under oxygen supply (Fig. 3B). Both of them demonstrated enhanced current densities, respectively -1.33 (-0.2 V vs. SCE)
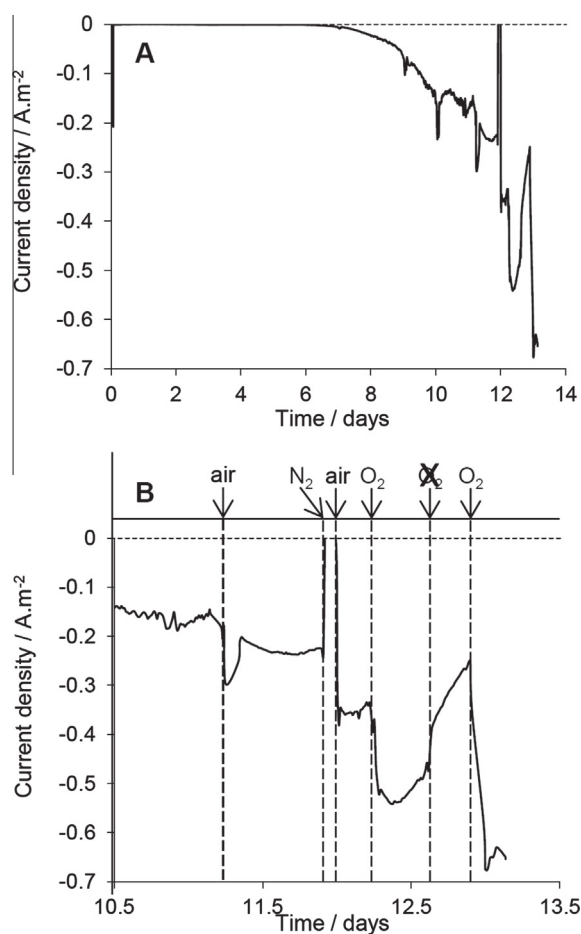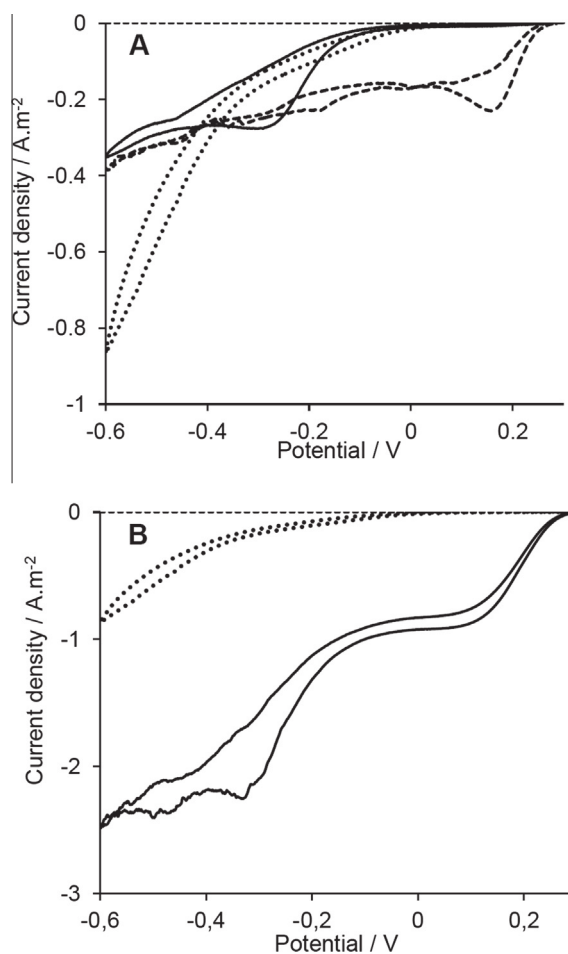

Fig. 2. Chronoamperometry recorded with the biocathode number 9 polarized at +0.1 V vs. SCE. A: whole experiment. B: detailed view focused on the last three days of experiment with the sequence of different gases supplied to the reactor.

Fig. 3. Cyclic voltammetries realized with biocathode number 9 polarized at +0.1 V vs. SCE. A: quiescent conditions, day 0 (dotted line); day 7 (plain line); day 11 (dashed line). B: quiescent conditions, day 0 (dotted line); with oxygen supply, day 13, (plain line).

and -0.92 A m^{-2} (+0.2 V vs. SCE), confirming that they were both related to oxygen reduction.

The progressive increase of the reductive current observed on Fig. 2 at +0.1 V vs. SCE was then attributable to the development of the redox signal at +0.2 V (Fig. 3), when redox system at -0.2 V did not produced any current (its potential, -0.2 V, being lower than the polarization potential, 0.1 V vs. SCE). Forming the oxygen-reducing bio-cathode at higher potential (+0.1 V vs. SCE) was thus of benefit, conferring it the ability to reduce oxygen at higher potential.

All the cathodes implemented within this study rapidly exhibited a capacity to produce a reductive current on cyclic voltammograms at potential lower than -0.2 V vs. SCE. However, the progressive apparition of a redox system able to interact with the cathode at a potential of +0.2 V vs. SCE was recorded on 4 electrodes (electrodes 6, 7, 8, 9) among the 5 poised at +0.1 vs. SCE. The difference in voltammetric signals recorded depending on the polarization potential likely corresponds to a change in the electron transfer mechanisms; such phenomenon was previously reported by Milner et al. (2014). Contrary to these authors, however, coexistence of two reductive signals was observed here with the highest potential (0.1 V vs. SCE = 342 mV vs. SHE), when they got two signals at the lowest potential (97 mV vs. SHE). The present experiments, however, clearly evidenced the signals relation to oxygen reduction, when the relation of one of Milner's signal to this reaction seemed dubious, as its current production was unaffected by oxygen depletion in the medium (Milner et al., 2014). To our knowledge, this study evidenced for the first time a change in behavior of electroactive biofilms toward oxygen reduction, depending on the applied potential. It suggested an adaptation of the biofilm and the development of an electroactive microbial community able to reduce oxygen at a high potential.

3.3. 16S rDNA tags pyrosequencing

To investigate the influence of cathode potential on microbial diversity and communities' composition, cathodic biofilms and populations of suspended bacteria were analyzed by 16S rDNA tags pyrosequencing at the end of the experiment for reactors 1, 2, 4, 6, 7, 8, 9 and 10. 94390 pyrotags were obtained from the variable region V1-3 of bacterial 16S. After trimming, sorting, and quality control, 68% of these sequences (64,153), with an average read length of 414 bp, remained and were used for the analysis. The sequences were clustered into 2295 operational taxonomic units (OTUs) at 3% distance threshold.

3.3.1. Diversity indexes

The number of OTUs, chao1, Shannon index and Simpson index of diversity were calculated for each sample and are shown in Supplementary Material (Table S1). Samples from biofilms on electrodes are notated E1–E10 and samples from liquid media are notated M1–M10.

The mean value of Shannon index (H) for all samples was 6.23 ($\pm$ 0.86) and the mean value of Simpson index of diversity (1-D) was 0.92 ($\pm$ 0.08). Both values were relatively high, in particular the Shannon index, which is in the same range as the one measured for different wastewaters (Wang et al., 2012), indicating no strong selection in most of the systems. However E6 and E9 exhibited low diversity with H index of 4.65 and 4.44 respectively and 1-D index of 0.79 and 0.75 indicating that the community was dominated by few OTUs. Given that these two electrodes exhibited the highest performances at +0.1 V vs. SCE, the dominant OTUs in their biofilm might constitute an interesting community for oxygen reduction at high potential. We thus further analyzed the sequences by assigning taxonomy with the RDP classifier.

3.3.2. Taxonomy

Barplots of relative abundances for bacterial orders are shown on Fig. 4. The relative abundances for electrode samples (E1–E10) appear in the upper part, while they appear in the lower part of the figure for electrolyte samples (M1–M10). Major bacterial orders are different in the two graphs, with, for example, high proportions of unidentified γ-proteobacteria found in several biofilms but not in electrolyte, while Legionellales are, on the contrary, only found in electrolytes. To identify more precisely OTUs that were statistically overabundant on the eight electrodes in comparison with OTUs found in the seven media we used edgeR package combined with phyloseq in R software environment (McMurdie and Holmes, 2013; Robinson et al., 2010). Overabundant OTUs for biofilms (characterized by a positive log fold change as calculated by edgeR) and with false discovery rate below 1E−2 are shown on Table 2 together with their relative abundances in biofilms (see Supplementary Material Table S2 for statistical values calculated with edgeR for selected OTUs). Interestingly, unidentified γ-proteobacteria (OTUs 1411 and 1780) appear to be selected specifically on electrode at +0.1 V while bacilli (OTUs 963, 681, 1526 and 1443) are enriched on electrodes at -0.4 V. Incidentally, it can be noted that OTU 1788 identified as *Acinetobacter* was found on all electrodes. Several *Acinetobacter* species have already been reported as able to reduce oxygen on cathodes (Rosenbaum et al., 2011), but they probably played only a minor role in the electroactivity of the biocathodes as the corresponding OTU had only very low abundances in all biofilms.

3.3.3. Overabundant OTUs on -0.4 V electrodes

On electrodes poised at -0.4 V vs. SCE, overabundant OTUs were assigned to order Bacillales (Table 2), in particular genera *Bacillus* and *Aneurinibacillus* were identified. Different species of *Bacillus* are known as electroactive bacteria (Nimje et al., 2009; Zhang et al., 2012a) and *Bacillus subtilis* has been shown to catalyze oxygen reduction on oxygen reducing biocathodes (Cournet et al., 2010b) these species may thus explain the oxygen reduction capacity of electrodes 2 and 4. However their abundances are very low on electrode 1 (Table 2), thus its electroactivity may rather be explained by other potential electroactive oxygen reducing bacteria, such as Rhizobiales or Pseudomonadales (Cournet et al., 2010a; Wang et al., 2013) that were abundant in its biofilm (Fig. 4).

3.3.4. Overabundant OTUs on +0.1 V electrodes

On electrodes poised at +0.1 V vs. SCE, the two OTUs 1411 and 1780 belonging to unidentified orders of γ-proteobacteria were specifically found and highly abundant except on E10 (Table 2). Interestingly the abundance of these γ-proteobacteria was correlated to current densities (Supplementary Material Figure S2) suggesting a key role in biofilm electroactivity. For the highest performing electrodes, E6 and E9, OTUs 1780 or 1411 encompass almost half of retrieved sequences, further supporting a possible competitive advantage for oxygen reduction at high potential.

γ-proteobacteria were found in abundance in other studies on biocathodes reducing oxygen at high potential (Rothballer et al., 2015; Strycharz-Glaven et al., 2013; Wang et al., 2015; Xia et al., 2012). Several different taxonomic assignations were mentioned: genera *Thiorhodospira* and *Alkalilimnicola* (Xia et al., 2012), genus *Marinobacter* (Strycharz-Glaven et al., 2013; Wang et al., 2015), family Chromatiaceae (Wang et al., 2015), unidentified γ-proteobacteria (Rothballer et al., 2015). The precise taxonomic position of corresponding bacteria however often remained unclear and the RDP classifier was here unable to resolve the precise taxonomic affiliation of OTUs 1411 and 1780.
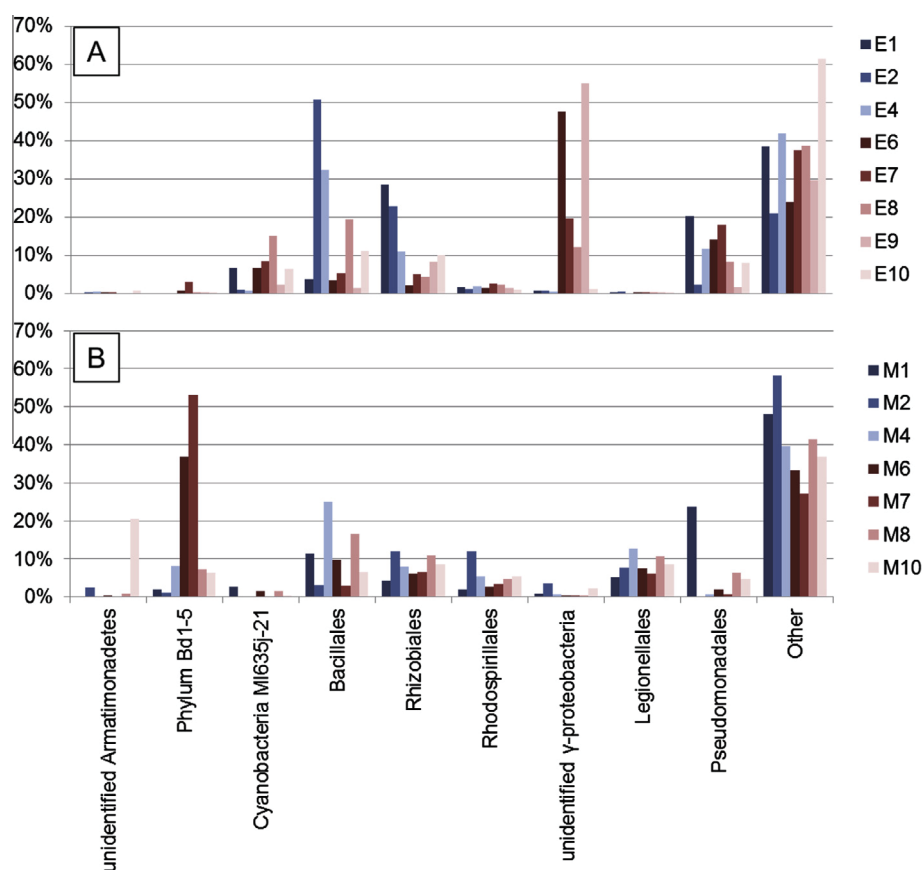
Fig. 4. Bacterial community composition on electrodes (A) and in liquid media (B). Relative abundances are shown only for orders representing at least 10% of sequences in at least one sample. Data are missing for medium sample M9 because we were not able to extract enough DNA to perform pyrosequencing on this sample.

Table 2
OTUs detected as overabundant on the electrodes in comparison to surrounding media with a false discovery rate below 1E−2. The first column indicates OTU IDs, the next three columns indicate taxonomic assignations obtained from the RDP classifier and the last eight columns give relative abundances computed from 16S sequence abundances for electrodes 1, 2, 4 polarized at −0.4 V vs. SCE and electrodes 6, 7, 8, 9, 10 polarized at +0.1 V vs. SCE.

OTU ID	Class	Order	Genus	−0.4 V vs. SCE			+0.1 V vs. SCE				
				E1	E2	E4	E6	E7	E8	E9	E10
1411	γ-Proteobacteria	Unidentified	Unidentified	0.0%	0.0%	0.0%	0.0%	16.6%	0.0%	49.8%	0.2%
1780				0.0%	0.0%	0.1%	45.2%	0.0%	8.7%	0.0%	0.6%
1788		Pseudomonadales	*Acinetobacter*	0.4%	0.8%	0.9%	0.3%	0.2%	0.3%	0.3%	0.5%
963	Bacilli	Bacillales	*Aneurinibacillus*	0.3%	6.2%	4.5%	0.6%	0.5%	0.3%	0.4%	0.7%
681			*Bacillus*	0.3%	6.7%	3.9%	0.3%	0.6%	0.4%	0.1%	0.6%
1526			Unidentified	0.2%	2.8%	1.2%	0.1%	0.2%	0.0%	0.0%	0.7%
1443			*Bacillus*	0.7%	4.4%	2.9%	0.3%	0.7%	0.0%	0.2%	0.7%

The dark red to white colors correspond to high to low relative abundances values.

3.3.5. Resolving the taxonomic position of unidentified γ-proteobacteria found on highly electroactive electrodes polarized at +0.1 V vs. SCE

In order to assess more precisely the position of these microorganisms in the bacterial tree and to try to understand their metabolism, a phylogeny of γ-proteobacterial sequences was reconstructed (Supplementary Material Figure S3) including sequences JN802222 and JN802218 from Genbank published by Xia et al. to which representative sequences of OTUs 1411 and 1780 were 96% and 97% identical, respectively. According to the maximum likelihood tree, the corresponding bacteria belong to family Ectothiorhodospiraceae, a family of purple sulfur bacteria producing sulfur globules outside of their cells (Ghosh and Dam, 2009) constituting together with Chromatiaceae the bacterial order of Chromatiales. Such chemolithoautotrophic sulfur-oxidizing bacteria may indeed include interesting bacteria for bioelectrochemical applications as they are able to oxidize sulfur and sometimes other inorganic compounds such as arsenite using oxygen as an electron acceptor and carbon dioxide as sole carbon source (Hoeft et al., 2007; Sorokin and Kuenen, 2005).

3.4. Metagenome of the Ectothiorhodospiraceae dominated biofilm from electrode 9

To further characterize the biological composition and functional potential of microbial community from the oxygen reducing biocathodes formed during this experiment, the biofilm of the most efficient electrode (E9), for which 49.8% of 16S ribotags

sequences were assigned to Ectothiorhodospiraceae (OTU 1411), was subjected to whole-metagenome sequencing. Biocathode metagenome sequencing resulted in approximately 2.8E6 filtered raw reads that allowed identifying 6.0E5 protein features and 1.7E3 rRNA features using online pipeline MG-RAST (Meyer et al., 2008). Rarefaction curves (Supplementary Material Figure S4) for species and functions indicated a reasonable coverage for the metagenome. rRNA reads were analyzed with the QIIME pipeline (Caporaso et al., 2010) to determine the taxonomic composition of the biofilm. The results at the order taxonomic level are shown in Supplementary Material (Fig. S5). They are similar to results obtained from pyrotags sequencing except sequences attributed to Thermoanaerobacterales that were quite abundant among pyrotags (6%) but rare among metagenomic rRNA reads (0.06%).

3.4.1. Identification of Taxon Specific Gene Annotations (TSGA) for Ectothiorhodospiraceae

The analysis of the performances of the ten oxygen reducing electrodes together with 16S pyrotag sequencing indicated that only few bacterial phylotypes affiliated to Ectothiorhodospiraceae (OTUs 1780 and 1411) were probably implicated in oxygen reduction at high potential on the electrodes. As genes implicated in oxygen reduction on biocathodes are not known, we thus decided to investigate gene annotations that were specific to family Ectothiorhodospiraceae and we purposely developed an approach for the identification of Taxon Specific Gene Annotations (TSGA). For that, we determined an Ectothiorhodospiraceae specificity index by computing, for each gene annotation, the ratio of its abundance in the Ecothiorhodospiraceae gene annotation pool to its total abundance in the metagenome. A specificity of 1 thus indicates annotations that are only found in Ectothiorhodospiraceae, and specificity of 0 indicates those that are not found in Ectothiorhodospiraceae but in other families. Plots of distributions of specificity values for different Subsystem classification Level 1 categories are shown in Supplementary Material (Fig. S6). The functional category "Respiration" was of particular interest to us, as it groups numerous annotations implicated in electron transfer that may help to understand the metabolism of oxygen reduction on a biocathode. The distribution of its specificity values was bimodal with a group of non-specific annotations (low specificity values) and a group of highly specific ones (high specificity values) that allowed us to choose a discriminant threshold specificity value of 0.55 (cf. Supplementary Material Fig. S7). Annotations from all categories with specificity values above the threshold (Supplementary Material Fig. S8) were then selected for further analysis (Supplementary Material Table S3). These correspond to the overall ~5% most specific ones. Among these annotations, those belonging to categories "Respiration" and "Carbohydrates" from Subsystem classification Level 1 revealed highly interesting functions and are shown in Table 3.

3.4.2. Annotations specific to Ectothiorhodospiraceae associated with electron transfer and energy conservation

Genes implicated in extracellular electron transfer on biocathodes and associated metabolisms are not known, but eight of the ten annotations from category "Respiration" may give clues about electron transfer mechanisms for cathodic oxygen reduction by Ectothiorhodospiraceae. They include two subunits of a cytochrome-c3 hydrogenase. The corresponding sequences are related to several small and large subunits of archaeal and bacterial hydrogenases (Pedroni et al., 1995), in particular to a sulfide dehydrogenase found in *Pyrococcus furiosus* that appears to catalyze the reduction of different substrates including oxygen (Ma and Adams, 1994). The other type of cytochrome identified (cytochrome b-556) is an electron carrier anchoring heme with transmembrane subunits (Ruprecht et al., 2009) that may be implicated in extracellular electron transfer. The two subunits of CoB–CoM heterodisulfide reductase correspond to genes hdrB and hdrC which code for proteins part of a membrane bound H_2 reductase complex in methanogens. They are implicated in electron bifurcation mechanism via CoB–CoM heterodisulfide complex coupling the anabolic and the catabolic processes (Costa et al., 2010). Finally three annotations are associated with a carbon monoxide dehydrogenase complex. It may be involved in reduction of CO_2 to CO, a first step for carbon dioxide fixation in the Wood–Ljungdahl pathway. In addition, the list encompasses an ATP synthase that may generate proton motive force for energy conservation. The possible role of the sulfite reductase (EC 1.8.99.3) however remains unclear.

3.4.3. Annotations specific to Ectothiorhodospiraceae associated with carbon fixation

Wang et al. already illustrated how γ-proteobacteria express genes implicated in carbon dioxide fixation on a cathode poised at high potential (Wang et al., 2015). Accordingly, for electrode 9 poised at +0.1 V, the increase of current with time associated to the development of cyclovoltammetric redox signal at +0.2 V, indicate a possible autotrophic growth of electroactive microbes. Metagenomic results confirm that Ectothiorhodospiraceae may be implicated in carbon dioxide fixation in the biofilm on electrode 9. Indeed five specific annotations from category "Carbohydrates" plus three specific annotations from category "Respiration" are related to carbon dioxide fixation. Beside the three abovementioned functions related to the carbon monoxide dehydrogenase complex, two of the specific functions detected are associated to carboxysome synthesis that allows efficient capture of CO_2 (shell protein CsoS1 and putative carboxysome peptide B) (Berg, 2011),

Table 3
Subsystems annotations from categories "Respiration" and "Carbohydrates" specific to Ectothiorhodospiraceae (with specificity value above 0.55 threshold value).

Level 1	Level 2	Level 3	Function	Specificity
Respiration	ATP synthases	F0F1-type ATP synthase	ATP synthase delta chain (EC 3.6.3.14)	0.64
	Electron accepting reactions	Anaerobic respiratory reductases	CoB–CoM heterodisulfide reductase subunit B (EC 1.8.98.1)	0.65
			CoB–CoM heterodisulfide reductase subunit C (EC 1.8.98.1)	0.71
			Sulfite reductase, dissimilatory-type gamma subunit (EC 1.8.99.3)	0.75
	Electron donating reactions	CO dehydrogenase	Carbon monoxide dehydrogenase F protein	0.84
			Carbon monoxide dehydrogenase G protein	0.9
			Carbon monoxide dehydrogenase large chain (EC 1.2.99.2)	0.67
		Hydrogenases	Cytochrome-c3 hydrogenase alpha chain	0.88
			Cytochrome-c3 hydrogenase delta chain	0.8
		Succinate dehydrogenase	Succinate dehydrogenase cytochrome b-556 subunit	0.64
Carbohydrates	CO₂ fixation	CO₂ uptake, carboxysome	Carboxysome shell protein CsoS1	0.92
			Putative carboxysome peptide B	0.99
			Rubisco activation protein CbbO	0.84
			Rubisco activation protein CbbQ	0.83
		Photorespiration (oxidative C2 cycle)	Glycine dehydrogenase (EC 1.4.4.2)	0.55

two other are associated with RubisCO assembly (proteins CbbO and CbbQ) and finally the glycine dehydrogenase is implicated in Calvin-Benson cycle (Berg, 2011).

4. Conclusion

The influence of cathode polarization on microbial community structure and oxygen reducing activity was here documented in details. The selection of Ectothiorhodospiraceae on biocathodes efficiently reducing oxygen at high potential was evidenced. The identification of their Taxon Specific Gene Annotations (TSGA) on shotgun metagenomic data revealed that they harbor several specific genes possibly involved in O_2 reduction, energy conservation, electron transfer and CO_2 fixation. These microorganisms thus exhibit an original association of genetic features that explains their selection in the particular ecological niche constituted by a biocathode polarized at high potential in an electrolyte with little bioavailable organic carbon.

Conflict of interest

The authors declare no conflict of interest.

Acknowledgements

Appendix A. Supplementary data

Supplementary data associated with this article can be found, in the online version, at http://dx.doi.org/10.1016/j.biortech.2016.04.087.

References

Berg, I.A., 2011. Ecological aspects of the distribution of different autotrophic CO_2 fixation pathways. Appl. Environ. Microbiol. 77, 1925–1936.

Caporaso, J.G., Kuczynski, J., Stombaugh, J., Bittinger, K., Bushman, F.D., Costello, E.K., Fierer, N., Pena, A.G., Goodrich, J.K., Gordon, J.I., Huttley, G.A., Kelley, S.T., Knights, D., Koenig, J.E., Ley, R.E., Lozupone, C.A., McDonald, D., Muegge, B.D., Pirrung, M., Reeder, J., Sevinsky, J.R., Turnbaugh, P.J., Walters, W.A., Widmann, J., Yatsunenko, T., Zaneveld, J., Knight, R., 2010. QIIME allows analysis of high-throughput community sequencing data. Nat. Methods 7, 335–336.

Cercado, B., Byrne, N., Bertrand, M., Pocaznoi, D., Rimboud, M., Achouak, W., Bergel, A., 2013. Garden compost inoculum leads to microbial bioanodes with potential-independent characteristics. Bioresour. Technol. 134, 276–284.

Cole, J.R., Wang, Q., Cardenas, E., Fish, J., Chai, B., Farris, R.J., Kulam-Syed-Mohideen, A.S., McGarrell, D.M., Marsh, T., Garrity, G.M., Tiedje, J.M., 2009. The ribosomal database project: improved alignments and new tools for rRNA analysis. Nucl. Acids Res. 37, D141–D145.

Costa, K.C., Wong, P.M., Wang, T.S., Lie, T.J., Dodsworth, J.A., Swanson, I., Burn, J.A., Hackett, M., Leigh, J.A., 2010. Protein complexing in a methanogen suggests electron bifurcation and electron delivery from formate to heterodisulfide reductase. Proc. Natl. Acad. Sci. USA 107, 11050–11055.

Cournet, A., Berge, M., Roques, C., Bergel, A., Delia, M.L., 2010a. Electrochemical reduction of oxygen catalyzed by Pseudomonas aeruginosa. Electrochim. Acta 55, 4902–4908.

Cournet, A., Delia, M.L., Bergel, A., Roques, C., Berge, M., 2010b. Electrochemical reduction of oxygen catalyzed by a wide range of bacteria including Gram-positive. Electrochem. Commun. 12, 505–508.

Erable, B., Feron, D., Bergel, A., 2012. Microbial catalysis of the oxygen reduction reaction for microbial fuel cells: a review. Chemsuschem 5, 975–987.

Ghosh, W., Dam, B., 2009. Biochemistry and molecular biology of lithotrophic sulfur oxidation by taxonomically and ecologically diverse bacteria and archaea. Fems Microbiol. Rev. 33, 999–1043.

Guindon, S., Gascuel, O., 2003. A simple, fast, and accurate algorithm to estimate large phylogenies by maximum likelihood. Syst. Biol. 52, 696–704.

Hoeft, S.E., Blum, J.S., Stolz, J.F., Tabita, F.R., Witte, B., King, G.M., Santini, J.M., Oremland, R.S., 2007. Alkalilimnicola ehrlichii sp. nov., a novel, arsenite-oxidizing haloalkaliphilic gammaproteobacterium capable of chemoautotrophic or heterotrophic growth with nitrate or oxygen as the electron acceptor. Int. J. Syst. Evol. Microbiol. 57, 504–512.

Liang, P., Fan, M.Z., Cao, X.X., Huang, X., 2009. Evaluation of applied cathode potential to enhance biocathode in microbial fuel cells. J. Chem. Technol. Biotechnol. 84, 794–799.

Logan, B.E., 2009. Exoelectrogenic bacteria that power microbial fuel cells. Nat. Rev. Microbiol. 7, 375–381.

Ma, K., Adams, M.W., 1994. Sulfide dehydrogenase from the hyperthermophilic archaeon Pyrococcus furiosus: a new multifunctional enzyme involved in the reduction of elemental sulfur. J. Bacteriol. 176, 6509–6517.

McMurdie, P.J., Holmes, S., 2013. phyloseq: An R package for reproducible interactive analysis and graphics of microbiome census data. Plos One 8 (4), e61217. http://dx.doi.org/10.1371/journal.pone.0061217.

Meyer, F., Paarmann, D., D'Souza, M., Olson, R., Glass, E.M., Kubal, M., Paczian, T., Rodriguez, A., Stevens, R., Wilke, A., Wilkening, J., Edwards, R.A., 2008. The metagenomics RAST server – a public resource for the automatic phylogenetic and functional analysis of metagenomes. BMC Bioinformatics 9, 386.

Milner, E., Scott, K., Head, I., Curtis, T., Yu, E., 2014. Electrochemical investigation of aerobic biocathodes at different poised potentials: evidence for mediated extracellular electron transfer. Chem. Eng. Trans. 41, 355–360.

Nimje, V.R., Chen, C.Y., Chen, C.C., Jean, J.S., Reddy, A.S., Fan, C.W., Pan, K.Y., Liu, H.T., Chen, J.L., 2009. Stable and high energy generation by a strain of Bacillus subtilis in a microbial fuel cell. J. Power Sources 190, 258–263.

Pedroni, P., Della Volpe, A., Galli, G., Mura, G.M., Pratesi, C., Grandi, G., 1995. Characterization of the locus encoding the [Ni–Fe] sulfhydrogenase from the archaeon Pyrococcus furiosus: evidence for a relationship to bacterial sulfite reductases. Microbiology 141 (Pt 2), 449–458.

Quast, C., Pruesse, E., Yilmaz, P., Gerken, J., Schweer, T., Yarza, P., Peplies, J., Glockner, F.O., 2013. The SILVA ribosomal RNA gene database project: improved data processing and web-based tools. Nucl. Acids Res. 41, D590–D596.

Rimboud, M., Desmond-Le Quemener, E., Erable, B., Bouchez, T., Bergel, A., 2015. The current provided by oxygen-reducing microbial cathodes is related to the composition of their bacterial community. Bioelectrochemistry 102, 42–49.

Robinson, M.D., McCarthy, D.J., Smyth, G.K., 2010. EdgeR: a bioconductor package for differential expression analysis of digital gene expression data. Bioinformatics 26, 139–140.

Rosenbaum, M., Aulenta, F., Villano, M., Angenent, L.T., 2011. Cathodes as electron donors for microbial metabolism: which extracellular electron transfer mechanisms are involved? Bioresour. Technol. 102, 324–333.

Rothballer, M., Picot, M., Sieper, T., Arends, J.B., Schmid, M., Hartmann, A., Boon, N., Buisman, C.J., Barriere, F., Strik, D.P., 2015. Monophyletic group of unclassified gamma-Proteobacteria dominates in mixed culture biofilm of high-performing oxygen reducing biocathode. Bioelectrochemistry 106, 167–176.

Ruprecht, J., Yankovskaya, V., Maklashina, E., Iwata, S., Cecchini, G., 2009. Structure of Escherichia coli succinate: quinone oxidoreductase with an occupied and empty quinone-binding site. J. Biol. Chem. 284, 29836–29846.

Sorokin, D.Y., Kuenen, J.G., 2005. Haloalkaliphilic sulfur-oxidizing bacteria in soda lakes. FEMS Microbiol. Rev. 29, 685–702.

Strycharz-Glaven, S.M., Glaven, R.H., Wang, Z., Zhou, J., Vora, G.J., Tender, L.M., 2013. Electrochemical investigation of a microbial solar cell reveals a nonphotosynthetic biocathode catalyst. Appl. Environ. Microbiol. 79, 3933–3942.

Ter Heijne, A., Strik, D.P.B.T.B., Hamelers, H.V.M., Buisman, C.J.N., 2010. Cathode potential and mass transfer determine performance of oxygen reducing biocathodes in microbial fuel cells. Environ. Sci. Technol. 44, 7151–7156.

Wang, X., Hu, M., Xia, Y., Wen, X., Ding, K., 2012. Pyrosequencing analysis of bacterial diversity in 14 wastewater treatment systems in China. Appl. Environ. Microbiol. 78, 7042–7047.

Wang, Z., Leary, D.H., Malanoski, A.P., Li, R.W., Hervey, W.J.T., Eddie, B.J., Tender, G.S., Yanosky, S.G., Vora, G.J., Tender, L.M., Lin, B., Strycharz-Glaven, S.M., 2015. A previously uncharacterized, nonphotosynthetic member of the Chromatiaceae is the primary CO_2-fixing constituent in a self-regenerating biocathode. Appl. Environ. Microbiol. 81, 699–712.

Wang, Z.J., Zheng, Y., Xiao, Y., Wu, S., Wu, Y.C., Yang, Z.H., Zhao, F., 2013. Analysis of oxygen reduction and microbial community of air-diffusion biocathode in microbial fuel cells. Bioresour. Technol. 144, 74–79.

Wei, J.C., Liang, P., Huang, X., 2011. Recent progress in electrodes for microbial fuel cells. Bioresour. Technol. 102, 9335–9344.

Xia, X., Sun, Y.M., Liang, P., Huang, X., 2012. Long-term effect of set potential on biocathodes in microbial fuel cells: electrochemical and phylogenetic characterization. Bioresour. Technol. 120, 26–33.

Zhang, J.W., Zhang, E.R., Scott, K., Burgess, J.G., 2012a. Enhanced electricity production by use of reconstituted artificial consortia of estuarine bacteria grown as biofilms. Environ. Sci. Technol. 46, 2984–2992.

Zhang, Y.P., Sun, J., Hu, Y.Y., Li, S.Z., Xu, Q., 2012b. Bio-cathode materials evaluation in microbial fuel cells: a comparison of graphite felt, carbon paper and stainless steel mesh materials. Int. J. Hydrogen Energy 37, 16935–16942.